IEEE Transactions on Quantum Engineering

Received December 3, 2020; revised June 10, 2021; accepted June 21, 2021; date of publication June 29, 2021; date of current version July 21, 2021.

*Digital Object Identifier 10.1109/TQE.2021.3093055*

# Identification of Time-Varying Decoherence Rates for Open Quantum Systems

**SHUIXIN XIAO[1,3], SHIBEI XUE[2] (Senior Member, IEEE), DAOYI DONG[3] (Senior Member, IEEE), AND JUN ZHANG[1,2] (Senior Member, IEEE)**

[1]UMich–SJTU Joint Institute, Shanghai Jiao Tong University, Shanghai 200240, China
[2]Key Laboratory of System Control and Information Processing, Ministry of Education, and the Department of Automation, Shanghai Jiao Tong University, Shanghai 200240, China
[3]School of Engineering and Information Technology, University of New South Wales, Canberra, ACT 2600, Australia

Corresponding author: Jun Zhang (zhangjun12@sjtu.edu.cn).

**ABSTRACT** Parameter identification of quantum systems is a fundamental task in developing practical quantum technology. In this article, we study the identification of time-varying decoherence rates for open quantum systems. Given the measurement data of local observables, this can be formulated as an optimization problem. We expand the unknown decoherence rates into Fourier series and take the expansion coefficients as optimization variables. We then convert it into a minimax problem and apply a sequential linear programming technique to solve it. Numerical study on a two-qubit quantum system with a time-varying decoherence rate demonstrates the effectiveness of our algorithm.

**INDEX TERMS** Identification algorithm, minimax problem, open quantum system, sequential linear programming.

## I. INTRODUCTION

In the past two decades, quantum information technology made significant progresses in a variety of fields such as quantum communication [1], quantum computation [2], quantum simulation [3], and quantum precision measurement [4]. In many of these applications, a fundamental question is to obtain accurate dynamical models of the underlying quantum systems as well as the environments with which they interact. For example, in quantum computation, accurate models are required to generate high-fidelity quantum operations. In quantum control, the knowledge of system models has direct impact on the system performance [5].

For a closed quantum system that has no interaction with the environment, its dynamics are entirely determined by the Hamiltonian, and thus, the system identification is all about Hamiltonian parameters' estimation [6]. In [7], the identifiability of a closed quantum system has been studied, that is, how much knowledge can be attained from the system. A tomography method has been extensively used to obtain the Hamiltonian of a chain of interacting spins [8]. The work in [9] utilizes the time traces of observable measurements to identify Hamiltonian parameters, and the corresponding identifiability problem is then studied in [10] and [11]. The work in [12] proposes an effective two-step optimization algorithm and shows that it has low computational complexity.

In reality, a quantum system usually interacts with its surroundings and, thus, is subject to an inevitable environment. These types of systems are called as open quantum systems. In many open quantum systems, the dynamics can be described by a Markov approximation, namely, the interaction time is so short that the information flows from the system to the environment in a unidirectional manner [13]. The identifiability of Markovian quantum systems has been studied in [15]. The work in [16] proposes a dynamical identification approach by using quantum trajectory. In [17], an algorithm is developed to estimate system parameters from a temporal record of measured data. The work in [18] applies continuous measurement methods to identify system structure.

In some other open quantum systems, when a time-scale separation between the system and the environment is not possible, the information can flow from the environment back into the system, which results in a non-Markovian open quantum system [13], [14]. Solid-state physics is a broad arena, where open quantum systems exhibiting

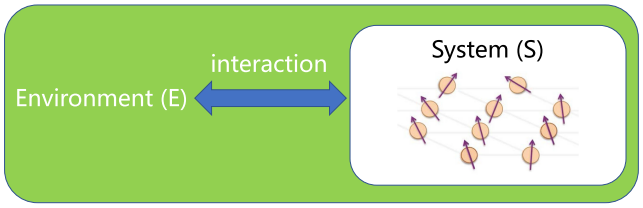


**FIGURE 1. Composite quantum system consisting of a subsystem *S* and its surrounding environment *E*.**

non-Markovian effects may appear [19]. To develop an accurate but efficient description of the system–environment interaction that goes beyond the Markov approximation, non-Markovian generalization of the Lindblad equation has been discussed in [13] and [29]. The work in [20] uses the system responses to an ensemble of measurements to identify the noises. In [21], a direct gradient algorithm has been developed to identify the non-Markovian environment for spin chains by time-local master equations. Other parameter estimation algorithms for quantum dynamics were proposed in [22]–[24].

The time-varying decoherence rates are important to understand the correlations of environments for Markovian and non-Markovian open quantum systems [21], [46]. In addition, we can measure the non-Markovianity of open quantum systems from time-varying decoherence rates [29], [30], which can give insights into the nature of non-Markovian effects.

In this article, we study the estimation of time-varying decoherence rates for open quantum systems. More specifically, we assume that we have access to local observable measurements and consider the case when the environment is characterized by time-varying decoherence rates. By expanding them in Fourier series, we formulate the identification into an optimization problem with Fourier expansion coefficients as optimization variables. We further transform it into a minimax problem and apply the sequential linear programming technique to solve it efficiently. A numerical study on a two-qubit quantum system with one decoherence rate demonstrates the efficacy of our algorithm.

The rest of this article is organized as follows. In Section II, a class of open quantum systems and its dynamic models are described. The identification problem is formulated in Section III. Section IV presents an identification algorithm based on sequential linear programming proposed to solve the parameter estimation problem of open quantum systems. Numerical examples are presented and the performance of the identification algorithm is compared in Section V. Section VI concludes this article.

## II. BACKGROUND AND PRELIMINARIES

Consider a composite quantum system, as shown in Fig. 1, which consists of a quantum subsystem $S$ and its surrounding environment $E$. In particular, $S$ is the physical system under investigation, e.g., a qubit network. This can be used to describe a wide range of applications in quantum information technology, e.g., spin wire that enables quantum state transfer [25]. We now briefly introduce the procedure to derive the dynamics of $S$ [26].

The physical state of the composite system can be described by a density operator $\rho_{se}(t)$, which is a positive-semidefinite Hermitian matrix with unity trace. This is a closed system, and its dynamics is governed by the von Neumann equation

$$\frac{d}{dt}\rho_{se}(t) = -i\,[H(t), \rho_{se}(t)] \tag{1}$$

where $i = \sqrt{-1}$, $[A, B] = AB - BA$, we set $\hbar = 1$, and $H(t)$ is the Hamiltonian and given by

$$H(t) = H_s(t) \otimes I_e + I_s \otimes H_e(t) + H_I(t).$$

Here, $H_s(t)$ is the Hamiltonian for the subsystem $S$, $H_e(t)$ is the Hamiltonian for the environment $E$, $H_I(t)$ is the interaction Hamiltonian between the subsystem $S$ and the environment $E$, $I$ is the identity matrix, and $\otimes$ denotes the tensor product.

The physical state of $S$ can be described by a reduced density operator $\rho_s \in \mathbb{C}^{N\times N}$, which is also a positive-semidefinite Hermitian matrix with unity trace, and it can be obtained from $\rho_{se}$ as $\rho_s = \mathrm{Tr}_s\,\rho_{se}$, where $\mathrm{Tr}_s$ is an operation known as the partial trace [2].

By employing the time-convolutionless projection operator technique [27], [28], we obtain that the dynamics of $\rho_s$ can be approximated by the following time-local quantum master equation [29]:

$$\begin{aligned}\dot{\rho}_s &= \mathcal{L}\rho_s = -i[H_s(t), \rho_s] + \mathcal{L}_D\rho_s \\ &= -i[H_s(t), \rho_s] \\ &\quad + \frac{1}{2}\sum_{j,l=1}^{N^2-1} r_{jl}(t)\left(\left[L_j, \rho_s L_l^\dagger\right] + \left[L_j\rho_s, L_l^\dagger\right]\right)\end{aligned} \tag{2}$$

where $\mathcal{L}_D$ is the Lindblad generator, $r_{jl}(t)$ are the time-varying decoherence rates that characterize the environment and $\bar{r}_{jl}(t) = r_{lj}(t)$, and $\{iL_j\}$ is an orthonormal basis for the Lie algebra $\mathfrak{su}(N)$, i.e., $L_j = L_j^\dagger$ with $\dagger$ denoting conjugate transpose. In the following sections, $\rho(t)$ refers to $\rho_s(t)$.

From (2), we can form the decoherence matrix $R$ as

$$R = \left\{r_{jl}(t)\right\}_{j,l=1}^{N^2-1}. \tag{3}$$

Because $R$ is Hermitian, it can be diagnolized as $R = U\Lambda U^\dagger$. We can also write it in the component form

$$r_{jl}(t) = \sum_k U_{jk}(t)\Delta_k(t)U_{lk}^\dagger(t) \tag{4}$$

where $\Delta_k(t)$ are the eigenvalues of $R$ and often referred as canonical decoherence rates.

Now, the environment $E$ is called *Markovian* if $\Delta_k(t)$ are nonnegative throughout the whole time evolution [29]. This

IEEE Transactions on Quantum Engineering

results in that the distinguishability between any two arbitrary initial states of $S$ decreases over the time. In the information interpretation, it indicates that the information flows from the system $S$ to the environment $E$ continuously, and there is no information flowing from $E$ back to $S$ [26]. This is the memoryless effect that is consistent with the definition of Markovian in the classical case.

On the other hand, the environment $E$ is called *non-Markovian* if there exists some time instant $t$ at which $\Delta_k(t)$ is negative [29]. This, in turn, indicates that the distinguishability between any two arbitrary initial states of $S$ might increase, and there may exist information flowing from $E$ back to $S$. This is the memory effect, and it is also consistent with the definition of non-Markovian in the classical case. For more details, see [13] and [26].

## III. PROBLEM FORMULATION

In this article, we assume that the Hamiltonian $H_s$ is known and time independent, and we are interested in identifying the time-varying decoherence rates $r_{jl}(t)$ from the measurement data of the quantum system as it evolves.

Introducing a coherence vector

$$x(t) = \begin{bmatrix} x_1(t) \\ \cdots \\ x_{N^2-1}(t) \end{bmatrix}$$

we can obtain a linear differential equation characterizing the complete quantum dynamics [21]

$$\dot{x}(t) = A(t)x(t) + b(t) \tag{5}$$

where the $j$th component of $x(t)$ is the expectation of the observable $L_j$, namely, $x_j(t) = \mathrm{Tr}L_j\rho(t)$, where $L_j$ is the same as (2). The detailed procedure of deriving $A(t) \in \mathbb{R}^{(N^2-1)\times(N^2-1)}$ and $b(t) \in \mathbb{R}^{(N^2-1)}$ from (2) can be found in [31] and [32]. Denote $\mathrm{Re}(x)$ as the real part of $x$ and $\mathrm{Im}(x)$ as the imaginary part of $x$. From [31] and [32], the $uv$th element of the matrix $A(t) \in \mathbb{R}^{(N^2-1)\times(N^2-1)}$ can be calculated as $A_{uv} = Q_{uv} + R_{uv}$, where

$$\begin{aligned} Q_{uv} &= \sum_{l=1}^{N^2-1} C_{lvu}h_l \\ R_{uv} &= -\frac{1}{4}\sum_{\substack{j,l,m=1 \\ (j\le l)}}^{N^2-1} (2-\delta_{jl})\,\mathrm{Re}\left(r_{jl}(t)\right)\left(C_{jmu}C_{lmv}+C_{lmu}C_{jmv}\right) \\ &\quad + \frac{1}{2}\sum_{\substack{j,l,m=1 \\ (j<l)}}^{N^2-1} \mathrm{Im}\left(r_{jl}(t)\right)\left(C_{lmu}d_{jmv} - C_{jmu}d_{lmv}\right) \end{aligned} \tag{6}$$

and the $u$th element of $b \in \mathbb{R}^{N^2-1}$ is

$$b_u = -\frac{2}{N}\sum_{\substack{j,l,m=1 \\ (j<l)}}^{N^2-1} \mathrm{Im}(r_{jl}(t))C_{jlu}. \tag{7}$$

All the structure constants $C_{jlm}$ and $d_{jlm}$ are real following from the Lie structure and the hermiticity of the decoherence matrix $R$ and $h_l$ are from the specific Hamiltonian [31], [32]. The explicit form of $C_{jlm}$ and $d_{jlm}$ can be found in [32, Appendix A.1] for $\mathfrak{su}(2)$, $\mathfrak{su}(3)$, and $\mathfrak{su}(4)$ for given basis, and we also give these structure constants of $\mathfrak{su}(4)$ in Appendix B. Note that because the decoherence rates $r_{jl}(t)$ are time varying, both $A(t)$ and $b(t)$ are time-varying real matrices [21].

In physical experiments, we can measure the expectation values of certain observables, e.g., local observables in a qubit network are frequently tracked as a function of time. These expectations can be expressed by a linear combination of the coherence vector $x$ and, thus, can be written as

$$y(t) = cx(t) \tag{8}$$

where $c$ is a time-independent matrix with $N^2-1$ columns. Equations (5) and (8) completely describe the dynamics of a qubit network subject to environments.

The dynamics of the coherence vector $x(t)$ is given in (5). Because it is possible that not all the elements in $x(t)$ are involved in the time evolution of the measured observable, we may find a reduced dynamical equation. This can be achieved by the following constructive procedure, which is a generalization of the filtration procedure in geometric control theory [33].

Since $x_j(t) = \mathrm{Tr}\,L_j\rho(t)$, we define the adjoint generator of dynamics through

$$\dot{x}_j = \mathrm{Tr}\left[L_j(\mathcal{L}\rho)\right] = \mathrm{Tr}\left[\left(\mathcal{L}^\dagger L_j\right)\rho\right]. \tag{9}$$

An iterative procedure can then be defined as

$$G_0 = \mathcal{M}, \quad G_i = \mathcal{L}^\dagger\left[G_{i-1}\right] \cup G_{i-1} \tag{10}$$

where $\mathcal{M}$ is the collection of unique basis elements that appear in the expansion of all the measured observables and

$$\mathcal{L}^\dagger\left[G_{i-1}\right] = \left\{L_j : \mathrm{tr}\left(L_j^\dagger\mathcal{L}^\dagger g\right) \neq 0, \text{ where } g \in G_{i-1}\right\}.$$

That is, at each iteration, we compute the adjoint evolution of each of the elements of $G_{i-1}$, and if the result has nonzero inner product with a basis element not already in $G_{i-1}$, this basis element is added to $G_i$. Since the dynamical system is finite dimensional, this iteration will saturate at a maximal set $\bar{G}$ after finite steps, which is referred as accessible set in [17]. More discussion about how to generate accessible sets can be found in [34].

This leads to a reduced dynamical equation

$$\begin{aligned} \dot{\tilde{x}}(t) &= \tilde{A}(t)\tilde{x}(t) + \tilde{b}(t) \\ y(t) &= \tilde{c}\tilde{x}(t) \end{aligned} \tag{11}$$

where $\tilde{A}(t)$, $\tilde{b}(t)$, and $\tilde{c}$ are submatrices of $A(t)$, $b(t)$, and $c$, respectively. This filtration procedure is important because it can significantly reduce the dimension of the quantum systems, as shown in [9], [10], and [17].

## IV. IDENTIFICATION ALGORITHM

Our objective is to use the time traces of the measured observable expectation values to estimate the unknown time-varying decoherence rates that characterize the environment.

The estimation setting we consider is as follows. Suppose that we prepare the qubit network at a given initial condition and let this system evolve for a fixed time duration $[0, T]$. We then measure a local observable at regular time instants $k\Delta t$ for some sampling period $\Delta t$ and let $K = T/\Delta t$. After repeating this measurement for multiple times and taking average, we obtain an approximation of the expectation value for the prescribed observable at all the sampling time instants, which is named time traces of system observables. The details of the measurement process can be found in [35]. Denote these measurement results as $y = [y(1), \ldots, y(K)]$. The estimation problem was formulated as an optimization problem in [21]

$$\min_{r_{jl}(t)} J = \frac{1}{2}\sum_{k=1}^{K} (\hat{y}(k) - y(k))^2 \tag{12}$$

where $\hat{y}(k)$ are the outputs generated by the estimated decoherence rate $r(t)$ from the dynamical equation (11).

In general, the time-varying decoherence rates $r_{jl}(t)$ are complex, and therefore, $\tilde{A}$ and $\tilde{b}$ depend on both real and imaginary parts of $r_{jl}(t)$. For brevity of presentation, we consider a simplified case when $\tilde{A}$ and $\tilde{b}$ are dependent on a single real decoherence rate $r(t)$. In general, if there are $n$ decoherence rates, we need to identify the real and imaginary parts for each of them, which amounts to $2n$ functions. As can be seen from later discussion on Fourier decomposition, the computational load grows linearly with number of decoherence rates, and thus, it is straightforward to extend the ensuing identification technique to the multiple $r_{jl}(t)$ case.

We use Fourier series decomposition to express $r(t)$ as a finite summation of harmonics

$$r(t) = a_0 + \sum_{m=1}^{M}[a_m \cos m\omega t + b_m \sin m\omega t] \tag{13}$$

where $\omega = \frac{2\pi}{T}$. We do not assume that $r(t)$ is periodic because we only need to identify it in a fixed time duration $[0, T]$. The expansion is truncated at a value $M$, which can be chosen so that most of the energy of decoherence rate stays within the limit $M\omega$. In real physical experiments, there usually exists an upper bound for the significant frequency components in a signal. If such information is known *a priori*, we may choose $M$ such that the expansion up to the $M$th order contains the major part of the energy spectrum. If there is no information about the frequency distribution, we can choose a large enough value of $M$ and then verify at a later time.

Note that Fourier series decomposition is widely used in many applications of physical systems. For instance, Niu *et al.* [36] used Fourier series decomposition to better estimate the total building energy consumption of heating, ventilation, and air conditioning. Chen *et al.* [37] developed a general model to characterize multicomponent chirp signals by using Fourier series.

For a given time-varying $r(t)$, there is generally no analytical method to solve (11). To obtain numerical solutions, we use a piecewise constant function to approximate $r(t)$. For simplicity, we use the same time gridding as in the local observable measurements, that is, $K$ equally distributed intervals $\{[t_k, t_{k+1}]\}_{k=0}^{K-1}$ each of length $\Delta t$ on the time duration $[0, T]$. On each interval $[t_k, t_{k+1}]$, assume that the decoherence rate $r(t)$ takes constant value, which is equal to that on the left boundary $t = t_k$:

$$r(k) = a_0 + \sum_{m=1}^{M}\left[a_m \cos mk\frac{2\pi}{K} + b_m \sin mk\frac{2\pi}{K}\right]. \tag{14}$$

Therefore, the matrices $\tilde{A}(t)$ and $\tilde{b}(t)$ in (11) become constant matrices $\tilde{A}_k$ and $\tilde{b}_k$ on the interval $[t_k, t_{k+1}]$, for $k = 0, 1, \ldots, K-1$. The time-varying (11) becomes a time-invariant equation

$$\begin{aligned}\dot{\tilde{x}}(t) &= \tilde{A}_k\tilde{x}(t) + \tilde{b}_k\\ \hat{y}(t) &= \tilde{c}\tilde{x}(t), \quad t \in [t_k, t_{k+1}]\end{aligned} \tag{15}$$

where $\tilde{A}_k$ and $\tilde{b}_k$ refer to $\tilde{A}(t_k)$ and $\tilde{b}(t_k)$, respectively. The solution of (15) can be obtained as

$$\tilde{x}_{k+1} = e^{\tilde{A}_k\Delta t}\tilde{x}_k + \int_0^{\Delta t} e^{\tilde{A}_k\tau}\tilde{b}_k d\tau \tag{16}$$

where $\tilde{x}_{k+1}$ and $\tilde{x}_k$ refer to $\tilde{x}(t_{k+1})$ and $\tilde{x}(t_k)$, respectively. Now, we can explicitly compute the output from a piecewise constant approximation of $r(t)$, as defined in (14).

Note that the optimization problem (12) uses a least mean square type of cost function, which sums up the difference between the real measurement $y(k)$ and the output $\hat{y}(k)$ generated by an estimated $r(k)$ at all the time instants $t_k$ and, thus, makes the optimization algorithm difficult to converge. To effectively estimate the decoherence rate, we transform it into a minimax problem, which instead minimizes the upper bound for all these individual errors. This makes it possible to reduce these errors simultaneously and solve the problem efficiently by using the sequential linear programming technique and, therefore, has smaller computational load and converges faster [38], [39].

Juxtaposing all the coefficients $a_0$, $a_m$, and $b_m$ into a vector, we obtain

$$p = [a_0, a_1, \ldots, a_M, b_1, \ldots, b_M]^T. \tag{17}$$

To identify $p$, we need to ensure $K \geq 2M + 1$, and we can obtain the following minimax problem:

$$\min_{p} \max_{k\in\{1,2,\ldots,K\}} J_k(p) \tag{18}$$

where

$$J_k(p) = \frac{1}{2}(\hat{y}(k) - y(k))^2. \tag{19}$$

The function $J_k$ measures the difference between $y(k)$ and $\hat{y}(k)$, and $\max_k J_k$ is the maximum error over all the time

IEEE Transactions on Quantum Engineering

instants $\{t_k\}_{k=1}^K$. When this maximum error is minimized, we achieve the goal of finding an approximate estimation of the decoherence rate.

Define $\gamma = \max\{J_k\}_{k=1}^K$. The minimax problem can be transformed into an equivalent form as

$$\min_p \gamma$$
$$\text{subject to} \quad J_1(p) \le \gamma, \ \ldots, \ J_K(p) \le \gamma. \tag{20}$$

Suppose that at the $j$th step in the iteration, the current estimation of the expansion coefficients $p$ is $p^j$. We want to determine a small correction term $\Delta p^j$ such that $p^{j+1} = p^j + \Delta p^j$ will reduce the maximum error. By first-order approximation, we have that

$$J_k(p^{j+1}) \approx J_k(p^j) + \nabla_{p^j}^T J_k(p^j) \Delta p^j. \tag{21}$$

Here, $\nabla_{p^j}^T J_k(p^j)$ is the gradient of $J_k(p^j)$ with respect to $p^j$, and it can be calculated as

$$\nabla_{p^j}^T J_k(p^j) = (\hat{y}(k) - y(k))\tilde{c}\frac{d\tilde{x}_k}{dp^j}. \tag{22}$$

The analytical procedure to compute $\frac{d\tilde{x}_k}{dp^j}$ is presented as follows.

Denote the $n$th element of $p$ as $p_n$ and we calculate the $n$th element of $\frac{d\tilde{x}_k}{dp}$, i.e., $\frac{d\tilde{x}_k}{dp_n}$. Taking derivatives of both sides of (16) yields

$$\frac{d\tilde{x}_{k+1}}{dp_n} = \frac{de^{\tilde{A}_k\Delta t}}{dp_n}\tilde{x}_k + e^{\tilde{A}_k\Delta t}\frac{d\tilde{x}_k}{dp_n} + \int_0^{\Delta t} \frac{de^{\tilde{A}_k\tau}}{dp_n} d\tau \, \tilde{b}_k + \int_0^{\Delta t} e^{\tilde{A}_k\tau} d\tau \, \frac{d\tilde{b}_k}{dp_n} \tag{23}$$

and the initial condition is $\frac{d\tilde{x}_0}{dp_n} = 0$. It is clear that the gradient at time instant $t_k$ depends only on gradient at the previous time instant $t_{k-1}$.

In this iterative calculation, we need to determine three terms, namely,

$$\frac{de^{\tilde{A}_k\Delta t}}{dp_n}, \quad \int_0^{\Delta t} \frac{de^{\tilde{A}_k\tau}}{dp_n} d\tau, \quad \text{and} \quad \frac{d\tilde{b}_k}{dp_n}.$$

Note that $\tilde{A}(t)$ and $\tilde{b}(t)$ are submatrices of $A(t)$ and $b(t)$, respectively. For the simplified case of $r(k)$ under investigation, we can write

$$\tilde{A}_k = \tilde{Q}_0 + r(k)\tilde{R}_0$$
$$\tilde{b}_k = r(k)\tilde{b}_0. \tag{24}$$

Rewrite (14) as $r(k) = p^T d^k$, where

$$d^k = \left[1 \ \cos k \ \ldots \ \cos Mk \ \sin k \ \ldots \ \sin Mk\right]^T.$$

Denote the $n$th element of $d^k$ as $d_n^k$. Now, we can rewrite (24) as

$$\tilde{A}_k = \tilde{Q}_0 + p^T d^k \tilde{R}_0 = \tilde{Q}_0 + \sum_{n=1}^{2M+1} p_n d_n^k \tilde{R}_0$$
$$\tilde{b}_k = p^T d^k \tilde{b}_0 = \sum_{n=1}^{2M+1} p_n d_n^k \tilde{b}_0. \tag{25}$$

To evaluate the derivative of a matrix exponential function with respect to a vector, we need the following formula [40]:

$$\frac{d}{dx} e^{(A+xB)t}\Big|_{x=0} = \int_0^t e^{Av} B e^{-Av} e^{At} dv. \tag{26}$$

Now, the first term $\frac{de^{\tilde{A}_k\Delta t}}{dp_n}$ can be obtained as

$$\frac{de^{\tilde{A}_k\Delta t}}{dp_n} = d_n^k \int_0^{\Delta t} e^{\tilde{A}_k v} \tilde{R}_0 e^{-\tilde{A}_k v} dv \cdot e^{\tilde{A}_k\Delta t}. \tag{27}$$

The second term $\int_0^{\Delta t} \frac{de^{\tilde{A}_k\tau}}{dp_n} d\tau$ is

$$\int_0^{\Delta t} \frac{de^{\tilde{A}_k\tau}}{dp_n} d\tau = d_n^k \int_0^{\Delta t} \int_0^{\tau} e^{\tilde{A}_k v} \tilde{R}_0 e^{-\tilde{A}_k v} dv \cdot e^{\tilde{A}_k\tau} d\tau. \tag{28}$$

And the third term $\frac{d\tilde{b}_k}{dp_n}$ is straightforward

$$\frac{d\tilde{b}_k}{dp_n} = d_n^k \tilde{b}_0. \tag{29}$$

We then apply a sequential linear programming algorithm as follows.

1) Choose an initial guess of the Fourier coefficient vector $p_0$.
2) At the $j$th iteration, compute $J_k(p^j)$ and $\nabla_{p^j}^T J_k(p^j)$;
3) Determine the increment $\Delta p^j$ from the following linear programming problem:

$$\min_{\Delta p^j} \gamma \tag{30}$$

subject to

$$\nabla_{p^j} J_1(p^j)\Delta p^j + J_1(p^j) \le \gamma$$
$$\vdots$$
$$\nabla_{p^j} J_K(p^j)\Delta p^j + J_K(p^j) \le \gamma.$$

4) Let $p^{j+1} = p^j + \Delta p^j$.
5) Repeat 2–4 until a desired convergence is reached.

The main advantage for this algorithm is that in each iteration, we only need to solve a linear programming problem, which accelerates the convergence. Then, we give the algorithm complexity analysis for our estimation algorithm. The main algorithm complexity is to solve the linear programming problem (30). The work in [41]–[43] has discussed the

algorithm complexity for the linear programming problem

$$\begin{aligned} &\min d^T x \\ &\text{s.t. } Dx \geq q \end{aligned} \tag{31}$$

where $D \in R^{m\times n}$, $q \in R^m$, and $d \in R^n$. An algorithm requires $O((m+n)^{1.5}nL)$ [43] in the worst case, where $m$ is the number of constraints and $n$ is the number of variables. The parameter $L$ is defined as

$$L = \log_2(1 + \det_{\max}) + \log_2 \xi + \log_2(m+n) \tag{32}$$

where $\det_{\max}$ denotes the largest absolute value of the determinant of any square submatrix of $\begin{bmatrix} d^T & 0 \\ D & q \end{bmatrix}$ and $\xi$ denotes the least common multiple of the denominators of all the numbers in the input [43]. We define $Y = [J_1(p^j), \ldots, J_K(p^j)]^T$, $\Pi_{kj} = \nabla^T_{p^j} J_k(p^j)$, $d = [0, \ldots, 0, 1]^T$. Then, (30) can be transformed as standard form like (31)

$$\begin{aligned} &\min d^T \begin{bmatrix} \Delta p^j \\ \gamma \end{bmatrix} \\ &\text{s.t. } \begin{bmatrix} -\Pi & \mathbf{1} \end{bmatrix} \begin{bmatrix} \Delta p^j \\ \gamma \end{bmatrix} \geq Y. \end{aligned} \tag{33}$$

Therefore, in each iteration, our algorithm complexity is $O((2M+K+2)^{1.5}(2M+2)L)$, where $K = \frac{T}{\Delta t}$ is the number of time intervals and $M$ is the Fourier expansion order. Now, some fast algorithms to solve sparsity linear programming problem have also been given in [44] and [45]. If the number of iterations is $N$, the total algorithm complexity is $O((2M+K+2)^{1.5}(2M+2)LN)$ in the worst case for our algorithm.

Note that our algorithm searches optimal solutions according to the gradient, and we might find local minimum and cannot obtain accurate estimate. Thus, we need to choose different initial guesses of the Fourier coefficient $p_0$ and repeat our algorithm to find the optimal local minimum.

## V. NUMERICAL EXAMPLES

In this section, we investigate the estimation of one time-varying decoherence rate by applying the algorithm derived in the preceding section.

Consider a system in which two qubits are coupled with $XY$ interaction, and the system *per se* is surrounded by a reservoir consisting of harmonic oscillators in the vacuum state. This two-qubit example can be used to describe the system of two two-level atoms interacting with an optical cavity, which is an important example to demonstrate the time-varying decoherence rate and non-Markovianity [46]. The corresponding time-local master equation can then be given as [46]

$$\dot{\rho}(t) = -i[H, \rho(t)] + \frac{r(t)}{2} \sum_{l=1}^{2} \left( [\sigma_-^l \rho(t), \sigma_+^l] + [\sigma_-^l, \rho(t)\sigma_+^l] \right). \tag{34}$$

In (34), the Hamiltonian $H$ can be written as

$$H = \sum_{l=1}^{2} \frac{\omega_l}{2} \sigma_z^l + \frac{g}{2}(\sigma_x^1 \sigma_x^2 + \sigma_y^1 \sigma_y^2) \tag{35}$$

where $\sigma_x$, $\sigma_y$, and $\sigma_z$ are Pauli matrices

$$\sigma_x = \begin{bmatrix} 0 & 1 \\ 1 & 0 \end{bmatrix}, \sigma_y = \begin{bmatrix} 0 & -i \\ i & 0 \end{bmatrix}, \sigma_z = \begin{bmatrix} 1 & 0 \\ 0 & -1 \end{bmatrix} \tag{36}$$

and $\sigma_\alpha^1 \sigma_\beta^2$ is the tensor product of $\sigma_\alpha$ on the first qubit and $\sigma_\beta$ on the second qubit. The ladder operators $\sigma_-^l$ and $\sigma_+^l$ are defined as

$$\begin{aligned} \sigma_-^l &= \frac{1}{2}(\sigma_x^l - i\sigma_y^l) \\ \sigma_+^l &= \frac{1}{2}(\sigma_x^l + i\sigma_y^l). \end{aligned}$$

For a particular system, let $g = 1$ GHz be the coupling strength between two qubits, and $\omega_1 = \omega_2 = 0.5$ GHz be the angular frequencies for these two qubits because in experimental conditions, these frequencies are usually in gigahertz. The decoherence rate $r(t)$ can be obtained from a damped Jaynes–Cummings model with detuning by using the time-convolutionless projection operator technique [46], and it can be written as

$$\begin{aligned} r(t) = {} & \frac{r_0 \lambda^2}{\lambda^2 + f^2} \left[ 1 - e^{-\lambda t} \left( \cos ft - \frac{f}{\lambda} \sin ft \right) \right] \\ & + \frac{r_0^2 \lambda^5 e^{-\lambda t}}{2(\lambda^2 + f^2)^3} \left\{ \left( 1 - 3\frac{f^2}{\lambda^2} \right) \left( e^{\lambda t} - e^{-\lambda t} \cos 2ft \right) \right. \\ & - 2\left( 1 - \frac{f^4}{\lambda^4} \right) \lambda t \cos ft + 4\left( 1 + \frac{h^2}{\lambda^2} \right) ft \sin ft \\ & \left. + \frac{f}{\lambda} \left( 3 - \frac{f^2}{\lambda^2} \right) e^{-\lambda t} \sin 2ft \right\} \end{aligned} \tag{37}$$

where the parameter $\lambda$ defines the spectral width of the atom–cavity coupling, and we choose $r_0 = 5$ GHz, $\lambda = 0.3\, r_0$, and $f = 8\,\lambda$ [46]. In the ensuing numerical study, this analytic expression can be used to generate measurement data for identification.

Assume that we measure the observable $\sigma_z$ for the first qubit, we can obtain the reduced coherence vector as

$$\tilde{x} = \left[ \left\langle \sigma_z^1 \right\rangle, \left\langle \sigma_z^2 \right\rangle, \left\langle \sigma_x^1 \sigma_x^2 \right\rangle, \left\langle \sigma_x^1 \sigma_y^2 \right\rangle, \left\langle \sigma_y^1 \sigma_x^2 \right\rangle, \left\langle \sigma_y^1 \sigma_y^2 \right\rangle \right]^T \tag{38}$$

IEEE Transactions on Quantum Engineering

where each element in $\tilde{x}$ is the expectation of an observable, e.g., $\langle\sigma_z^1\rangle = \mathrm{Tr}\sigma_z^1\rho$. The detailed procedure to derive the accessible set is given in Appendix A. Furthermore, we have

$$\tilde{A}(t) = \begin{bmatrix} -r(t) & 0 & 0 & -g & g & 0 \\ 0 & -r(t) & 0 & g & -g & 0 \\ 0 & 0 & -r(t) & -\omega_2 & -\omega_1 & 0 \\ g & -g & \omega_2 & -r(t) & 0 & -\omega_1 \\ -g & g & \omega_1 & 0 & -r(t) & -\omega_2 \\ 0 & 0 & 0 & \omega_1 & \omega_2 & -r(t) \end{bmatrix}$$

$$\tilde{b}(t) = \begin{bmatrix} -r(t) & -r(t) & 0 & 0 & 0 & 0 \end{bmatrix}^T$$

$$\tilde{c} = \begin{bmatrix} 1 & 0 & 0 & 0 & 0 & 0 \end{bmatrix}. \tag{39}$$

As discussed earlier, the truncation order $M$ can be determined by the energy spectrum of the decoherence rate. Here, we choose $M = 20$ as a tradeoff between numerical accuracy and convergence rate. The initial values of the Fourier coefficients are set as $a_0 = 0.01$ and all the other elements as 0, and the terminal time is $\gamma_0 T = 2.5$, and the step size $\Delta t$ is $2 \times 10^{-12}$ s. In this example, the frequency $f$ in $r(t)$ is 12 GHz; then, we have $\frac{2\pi}{f}/\Delta t \approx 1049$ steps in one oscillation period. In general, the larger the frequency $f$, the smaller the step size $\Delta t$. Moreover, the gradient computation can be further simplified.

From (39), we can write $\tilde{A}_k = \tilde{Q}_0 + r(k)\tilde{R}_0$, where

$$\tilde{Q}_0 = \begin{bmatrix} 0 & 0 & 0 & -g & g & 0 \\ 0 & 0 & 0 & g & -g & 0 \\ 0 & 0 & 0 & -\omega_2 & -\omega_1 & 0 \\ g & -g & \omega_2 & 0 & 0 & -\omega_1 \\ -g & g & \omega_1 & 0 & 0 & -\omega_2 \\ 0 & 0 & 0 & \omega_1 & \omega_2 & 0 \end{bmatrix}$$

$$\tilde{R}_0 = -I. \tag{40}$$

Equation (27) can then be simplified to

$$\frac{de^{\tilde{A}_k\Delta t}}{dp_n} = -d_n^k e^{\tilde{A}_k\Delta t}\Delta t = -d_n^k e^{-r(k)\Delta t} e^{\tilde{Q}_0\Delta t}\Delta t \tag{41}$$

and (28) is now

$$\begin{aligned} \int_0^{\Delta t} \frac{de^{\tilde{A}_k\tau}}{dp_n} d\tau &= -d_k^n \int_0^{\Delta t} e^{\tilde{A}_k\tau}\tau d\tau \\ &= -d_k^n \left(\Delta t e^{\tilde{A}_k\Delta t}\tilde{A}_k^{-1} - \left(e^{\tilde{A}_k\Delta t} - I\right)\tilde{A}_k^{-2}\right). \end{aligned} \tag{42}$$

The numerical results are shown in Fig. 2. The real time-varying decoherence rate $r(t)$ is plotted in blue solid, the initial guess $r_0(t)$ in black solid, and the estimated $\tilde{r}(t)$ in red dashed. This result demonstrates that the proposed algorithm can estimate the unknown decoherence rate to a satisfactory level.

In Fig. 3, we show how the cost function is reduced as the iteration proceeds, where $\gamma$ quantifies the upper bound of the errors between the measurements and the outputs from the estimated decoherence rate at all the time instants. It is clear that the minimax algorithm brings down the cost function

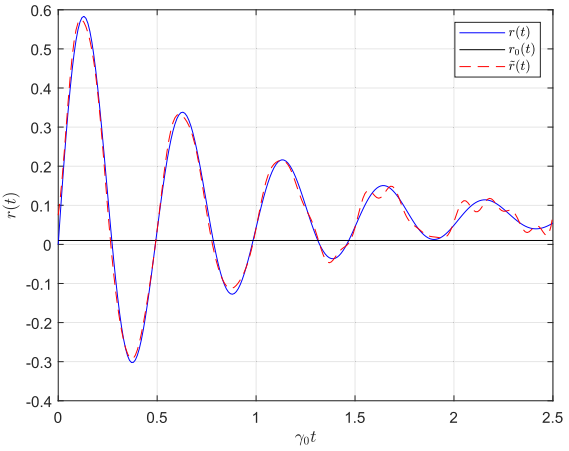


**FIGURE 2.** Estimation results of the decoherence rate, where $r(t)$ denotes the real time-varying decoherence rate, $r_0(t)$ is the initial guess, and $\tilde{r}(t)$ is the estimated decoherence rate.

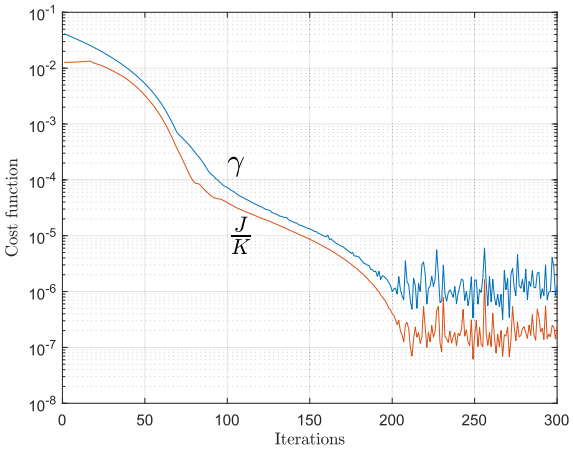


**FIGURE 3.** Cost function decreases as the iteration proceeds. Here, $\gamma$ is the maximum difference over all time instants and $\frac{J}{K}$ is the average mean squared error.

quickly. We also plot average mean squared error $\frac{J}{K}$ to show the gap between (12) and (18).

To ensure that the identified decoherence rate generates a real physical system, we need to check the complete positivity. Denote the flow of (34) as $\Phi_t$, i.e., $\rho(t) = \Phi_t(\rho(0))$. From [47, Th. 2], the linear map $\Phi_t$ is completely positive if and only if

$$(\Phi_t(E_{ik}))_{1\leqslant i,k\leqslant n} = \begin{bmatrix} \Phi_t(E_{11}) & \cdots & \Phi_t(E_{1n}) \\ \vdots & & \vdots \\ \Phi_t(E_{n1}) & \cdots & \Phi_t(E_{nn}) \end{bmatrix} \tag{43}$$

is positive semidefinite, where $E_{ik}$ is an $n \times n$ matrix with 1 at the $ik$th entry and 0 elsewhere. We then compute all the eigenvalues of $(\Phi_t(E_{ik}))_{1\leqslant i,k\leqslant n}$ with the identified decoherence rate over the entire time duration. The results are shown as in Fig. 4. It is clear that all these eigenvalues are nonnegative, and thus, the complete positivity is maintained.

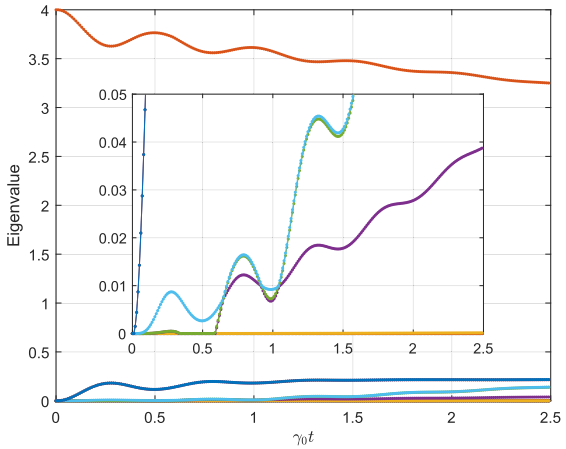


**FIGURE 4.** Eigenvalues of $(\Phi_t(E_{ik}))_{1\leqslant i,k\leqslant n}$ with the identified $\tilde{r}(t)$.

**TABLE I** Results of the Current Algorithm Versus Those in [21]

| | A algorithm in Ref. [21] | Current algorithm |
|---|---|---|
| Iterations | 2526 | 200 |
| Time consumed | 140.49 sec | 68.09 sec |

Xue *et al.* [21] studied the same model by engaging a direct gradient algorithm in the time domain. Setting the initial conditions and the termination conditions as the same, we can obtain the number of iterations and time consumed of these two algorithms, as shown in Table I. It is evident that the current algorithm uses fewer iterations and less time to achieve the same accuracy. Another least squares identification scheme was proposed in [48], and it can only be applied to one-qubit systems. Our algorithm can be applied to multiqubit systems.

The advantage of the current minimax algorithm is manifold. First, the direct gradient computation in [21] depends on all the past gradients and thus needs to keep track of all the information and consumes considerable computer time and storage. The minimax algorithm presented here uses an iterative procedure and, thus, has much smaller computational load and converges faster. Second, the size of optimization in [21] is the number of discretization steps in the evolved time duration. This is much larger than that in the minimax algorithm, which is the truncation order of Fourier expansion. Third, it is cumbersome to ensure smoothness of the signals in the time discretization setting, whereas in the Fourier expansion, it is naturally guaranteed.

## VI. CONCLUSION

In this article, we have developed an efficient algorithm to identify time-varying decoherence rates with local observable measurements and known time-independent subsystem's Hamiltonian, which can help us measure non-Markovianity of open quantum systems and understand system–environment correlations. By expanding the time-varying decoherence rates into Fourier series, we converted the identification task into a minimax optimization problem. The sequential linear programming technique was then applied to solve it quickly. Numerical study of a two-qubit model with one decoherence rate demonstrated the effectiveness of our algorithm. Comparing to existing algorithms, our algorithm converges fast and can be applied to multiqubit systems. In the future, we plan to apply the algorithm to more complicated models and further improve the convergence rate. We will also investigate the identifiablity of time-varying decoherence rates and the robustness of the proposed algorithm against noise.

## APPENDIX A
## ACCESSIBLE SET FOR OUR NUMERICAL EXAMPLE

To better explain the detailed procedure to derive the accessible set, we work out the accessible set for the numerical example as follows.

First, we measure the observable $\sigma_z^1$ and the initial accessible set is thus $G_0 = \{\sigma_z^1\}$. Derive the dynamics for $\langle\sigma_z^1\rangle$ as

$$\begin{aligned}\frac{d\langle\sigma_z^1\rangle}{dt} &= \mathrm{Tr}\left(\sigma_z^1\dot{\rho}\right) = \mathrm{Tr}\left(\sigma_z^1(-i[H,\rho])\right)\\ &\quad+\frac{r(t)}{2}\mathrm{Tr}\left(\sigma_z^1\left[\sigma_-^1\rho,\sigma_+^1\right]+\sigma_z^1\left[\sigma_-^1,\rho\sigma_+^1\right]\right)\\ &\quad+\frac{r(t)}{2}\mathrm{Tr}\left(\sigma_z^1\left[\sigma_-^2\rho,\sigma_+^2\right]+\sigma_z^1\left[\sigma_-^2,\rho\sigma_+^2\right]\right).\end{aligned} \tag{44}$$

The first term in the right-hand side of (44) can be derived as

$$\begin{aligned}&\mathrm{Tr}\left(\sigma_z^1(-i[H,\rho])\right) = -i\,\mathrm{Tr}\left(\sigma_z^1\left[\frac{\omega_1}{2}\sigma_z^1+\frac{\omega_2}{2}\sigma_z^2\right.\right.\\ &\quad\left.\left.+\frac{g}{2}\left(\sigma_x^1\sigma_x^2+\sigma_y^1\sigma_y^2\right),\rho\right]\right)\\ &= -\frac{ig}{2}\mathrm{Tr}\left(\sigma_z^1\sigma_x^1\sigma_x^2\rho-\sigma_z^1\rho\sigma_x^1\sigma_x^2\right)\\ &\quad-\frac{ig}{2}\mathrm{Tr}\left(\sigma_z^1\sigma_y^1\sigma_y^2\rho-\sigma_z^1\rho\sigma_y^1\sigma_y^2\right)\\ &= -\frac{ig}{2}\mathrm{Tr}\left(\sigma_z^1\sigma_x^1\sigma_x^2\rho-\sigma_x^1\sigma_x^2\sigma_z^1\rho\right)\\ &\quad-\frac{ig}{2}\mathrm{Tr}\left(\sigma_z^1\sigma_y^1\sigma_y^2\rho-\sigma_y^1\sigma_y^2\sigma_z^1\rho\right)\\ &= g\left\langle\sigma_y^1\sigma_x^2\right\rangle-g\left\langle\sigma_x^1\sigma_y^2\right\rangle.\end{aligned}$$

The second term is obtained

$$\begin{aligned}&\mathrm{Tr}\left(\sigma_z^1\left[\sigma_-^1\rho,\sigma_+^1\right]+\sigma_z^1\left[\sigma_-^1,\rho\sigma_+^1\right]\right)\\ &= \mathrm{Tr}\left(\left(2\sigma_+^1\sigma_z^1\sigma_-^1-\sigma_z^1\sigma_+^1\sigma_-^1-\sigma_+^1\sigma_-^1\sigma_z^1\right)\rho\right)=0\end{aligned}$$

and the third term is also calculated as

$$\begin{aligned}&\mathrm{Tr}\left(\sigma_z^1\left[\sigma_-^2\rho,\sigma_+^2\right]+\sigma_z^1\left[\sigma_-^2,\rho\sigma_+^2\right]\right)\\ &= \mathrm{Tr}\left(\left(2\sigma_+^2\sigma_z^1\sigma_-^2-\sigma_z^1\sigma_+^2\sigma_-^2-\sigma_+^2\sigma_-^2\sigma_z^1\right)\rho\right)\\ &= -\mathrm{Tr}\left(\left(2\sigma_z^1+2I\right)\rho\right)=-2\langle\sigma_z^1\rangle-2.\end{aligned}$$

IEEE Transactions on Quantum Engineering

Therefore, (44) becomes

$$\frac{d\left\langle\sigma_z^1\right\rangle}{dt} = g\left\langle\sigma_y^1\sigma_x^2\right\rangle - g\left\langle\sigma_x^1\sigma_y^2\right\rangle - r(t) - r(t)\left\langle\sigma_z^1\right\rangle. \quad (45)$$

Now, we need to find out the dynamics for $\left\langle\sigma_y^1\sigma_x^2\right\rangle$ and $\left\langle\sigma_x^1\sigma_y^2\right\rangle$, and the accessible set can be expanded to

$$G_1 = \left\{\sigma_z^1, \sigma_x^1\sigma_y^2, \sigma_y^1\sigma_x^2\right\}.$$

Proceeding further, we have

$$\begin{aligned}\frac{d\left\langle\sigma_x^1\sigma_y^2\right\rangle}{dt} &= \mathrm{Tr}\left(\sigma_x^1\sigma_y^2\dot{\rho}\right) = \mathrm{Tr}\left(\sigma_x^1\sigma_y^2(-i[H,\rho])\right)\\ &+ \frac{r(t)}{2}\mathrm{Tr}\left(\sigma_x^1\sigma_y^2\left[\sigma_-^1\rho, \sigma_+^1\right]\right.\\ &\left.+\sigma_x^1\sigma_y^2\left[\sigma_-^1, \rho\sigma_+^1\right]\right)\\ &+ \frac{r(t)}{2}\mathrm{Tr}\left(\sigma_x^1\sigma_y^2\left[\sigma_-^2\rho, \sigma_+^2\right]\right.\\ &\left.+\sigma_x^1\sigma_y^2\left[\sigma_-^2, \rho\sigma_+^2\right]\right). \quad (46)\end{aligned}$$

By calculating, we obtain

$$\begin{aligned}\mathrm{Tr}\left(\sigma_x^1\sigma_y^2(-i[H,\rho])\right) &= -\omega_1\left\langle\sigma_y^1\sigma_y^2\right\rangle + \omega_2\left\langle\sigma_x^1\sigma_x^2\right\rangle\\ &- g\left\langle\sigma_z^2\right\rangle + g\left\langle\sigma_z^1\right\rangle\\ \mathrm{Tr}\left(\sigma_x^1\sigma_y^2\left[\sigma_-^1\rho, \sigma_+^1\right] + \sigma_x^1\sigma_y^2\left[\sigma_-^1, \rho\sigma_+^1\right]\right) &= -\left\langle\sigma_x^1\sigma_y^2\right\rangle\\ \mathrm{Tr}\left(\sigma_x^1\sigma_y^2\left[\sigma_-^2\rho, \sigma_+^2\right] + \sigma_x^1\sigma_y^2\left[\sigma_-^2, \rho\sigma_+^2\right]\right) &= -\left\langle\sigma_x^1\sigma_y^2\right\rangle.\end{aligned}$$

Equation (46) can be simplified to

$$\begin{aligned}\frac{d\left\langle\sigma_x^1\sigma_y^2\right\rangle}{dt} &= -\omega_1\left\langle\sigma_y^1\sigma_y^2\right\rangle + \omega_2\left\langle\sigma_x^1\sigma_x^2\right\rangle\\ &- g\left\langle\sigma_z^2\right\rangle + g\left\langle\sigma_z^1\right\rangle - r(t)\left\langle\sigma_x^1\sigma_y^2\right\rangle. \quad (47)\end{aligned}$$

Similarly, we can obtain the dynamics for $\left\langle\sigma_y^1\sigma_x^2\right\rangle$ as

$$\begin{aligned}\frac{d\left\langle\sigma_y^1\sigma_x^2\right\rangle}{dt} &= \omega_1\left\langle\sigma_x^1\sigma_x^2\right\rangle - \omega_2\left\langle\sigma_y^1\sigma_y^2\right\rangle\\ &- g\left\langle\sigma_z^1\right\rangle + g\left\langle\sigma_z^2\right\rangle - r(t)\left\langle\sigma_y^1\sigma_x^2\right\rangle. \quad (48)\end{aligned}$$

Then, we need to find out dynamics for $\langle\sigma_z^2\rangle$, $\langle\sigma_x^1\sigma_x^2\rangle$, and $\left\langle\sigma_y^1\sigma_y^2\right\rangle$, and the accessible set becomes

$$G_2 = \left\{\sigma_z^1, \sigma_z^2, \sigma_x^1\sigma_x^2, \sigma_x^1\sigma_y^2, \sigma_y^1\sigma_x^2, \sigma_y^1\sigma_y^2\right\}.$$

The dynamics for these three terms can be derived as

$$\frac{d\left\langle\sigma_z^2\right\rangle}{dt} = -g\left\langle\sigma_y^1\sigma_x^2\right\rangle + g\left\langle\sigma_x^1\sigma_y^2\right\rangle - r(t) - r(t)\left\langle\sigma_z^2\right\rangle \quad (49)$$

$$\frac{d\left\langle\sigma_x^1\sigma_x^2\right\rangle}{dt} = -\omega_1\left\langle\sigma_y^1\sigma_x^2\right\rangle - \omega_2\left\langle\sigma_x^1\sigma_y^2\right\rangle - r(t)\left\langle\sigma_x^1\sigma_x^2\right\rangle \quad (50)$$

$$\frac{d\left\langle\sigma_y^1\sigma_y^2\right\rangle}{dt} = \omega_1\left\langle\sigma_x^1\sigma_y^2\right\rangle + \omega_2\left\langle\sigma_y^1\sigma_x^2\right\rangle - r(t)\left\langle\sigma_y^1\sigma_y^2\right\rangle. \quad (51)$$

In (49)–(51), all the observables are in $G_2$. Therefore, the iteration saturates at $G_2$.

Combining these equations of (45)–(51), we obtain the reduced dynamical equation

$$\begin{aligned}\dot{\tilde{x}}(t) &= \begin{bmatrix} -r(t) & 0 & 0 & -g & g & 0\\ 0 & -r(t) & 0 & g & -g & 0\\ 0 & 0 & -r(t) & -\omega_2 & -\omega_1 & 0\\ g & -g & \omega_2 & -r(t) & 0 & -\omega_1\\ -g & g & \omega_1 & 0 & -r(t) & -\omega_2\\ 0 & 0 & 0 & \omega_1 & \omega_2 & -r(t)\end{bmatrix}\tilde{x}(t)\\ &+ \begin{bmatrix} -r(t)\\ -r(t)\\ 0\\ 0\\ 0\\ 0\end{bmatrix} y = \left\langle\sigma_z^1\right\rangle \quad (52)\end{aligned}$$

where the reduced coherence vector is

$$\tilde{x} = \left[\left\langle\sigma_z^1\right\rangle, \left\langle\sigma_z^2\right\rangle, \left\langle\sigma_x^1\sigma_x^2\right\rangle, \left\langle\sigma_x^1\sigma_y^2\right\rangle, \left\langle\sigma_y^1\sigma_x^2\right\rangle, \left\langle\sigma_y^1\sigma_y^2\right\rangle\right]^T. \quad (53)$$

If we measure the observable $\sigma_x^1$, we can obtain the coherence vector in a similar filtration procedure as

$$\begin{aligned}\tilde{x} = &\left[\left\langle\sigma_x^1\right\rangle, \left\langle\sigma_y^1\right\rangle, \left\langle\sigma_x^2\right\rangle, \left\langle\sigma_y^2\right\rangle, \left\langle\sigma_x^1\sigma_z^2\right\rangle,\right.\\ &\left.\left\langle\sigma_y^1\sigma_z^2\right\rangle\left\langle\sigma_z^1\sigma_x^2\right\rangle, \left\langle\sigma_z^1\sigma_y^2\right\rangle\right]^T \quad (54)\end{aligned}$$

$$\dot{\tilde{x}}(t) = \begin{bmatrix} -r(t)/2 & -\omega_1 & 0 & 0 & 0 & 0 & 0 & g\\ \omega_1 & -r(t)/2 & 0 & 0 & 0 & 0 & -g & 0\\ 0 & 0 & -r(t)/2 & -\omega_2 & 0 & g & 0 & 0\\ 0 & 0 & \omega_2 & -r(t)/2 & -g & 0 & 0 & 0\\ -r(t) & 0 & 0 & g & -3r(t)/2 & -\omega_1 & 0 & 0\\ 0 & -r(t) & -g & 0 & \omega_1 & -3r(t)/2 & 0 & 0\\ 0 & g & -r(t) & 0 & 0 & 0 & -3r(t)/2 & -\omega_2\\ -g & 0 & 0 & -r(t) & 0 & 0 & \omega_2 & -3r(t)/2\end{bmatrix}\tilde{x}(t) \quad (55)$$

| $d_{jlm} = 1/\sqrt{2}$ | | $-1/\sqrt{2}$ | $1/\sqrt{6}$ | $1/\sqrt{3}$ | $-1/\sqrt{3}$ | $-2/\sqrt{6}$ | $-2\sqrt{3}$ |
|---|---|---|---|---|---|---|---|
| | 1, 9, 11 | 2, 9, 12 | 8, 9, 9 | 1, 1, 15 | 9, 9, 15 | 8, 13, 13 | 15, 15, 15 |
| | 1, 10, 12 | 3, 11, 11 | 8, 10, 10 | 2, 2, 15 | 10, 10, 15 | 8, 14, 14 | |
| | 2, 10, 11 | 3, 12, 12 | 8, 11, 11 | 3, 3, 15 | 11, 11, 15 | | |
| | 3, 9, 9 | 5, 9, 14 | 8, 12, 12 | 4, 4, 15 | 12, 12, 15 | | |
| | 3, 10, 10 | 7, 11, 14 | | 5, 5, 15 | 13, 13, 15 | | |
| $j, l, m$ | 4, 9, 13 | | | 6, 6, 15 | 14, 14, 15 | | |
| | 4, 10, 14 | | | 7, 7, 15 | | | |
| | 5, 10, 13 | | | 8, 8, 15 | | | |
| | 6, 11, 13 | | | | | | |
| | 6, 12, 14 | | | | | | |
| | 7, 12, 13 | | | | | | |

(60)

and its dynamical equation is described in (55), shown at bottom of the previous page.

For the last operator $\sigma_z^1\sigma_z^2$, its dynamics is

$$\frac{d\left\langle\sigma_z^1\sigma_z^2\right\rangle}{dt} = -r(t)\left\langle\sigma_z^1\right\rangle - r(t)\left\langle\sigma_z^2\right\rangle - 2r(t)\left\langle\sigma_z^1\sigma_z^2\right\rangle. \tag{56}$$

Therefore, the total dynamics for

$$x = \left[\left\langle\sigma_x^1\right\rangle, \left\langle\sigma_x^2\right\rangle, \cdots, \left\langle\sigma_z^1\sigma_z^2\right\rangle\right]^T$$

can be obtained from (52), (55), and (56).

## APPENDIX B
## EXPLICIT FORM FOR STRUCTURE CONSTANTS

Here, we give the structure constants $C_{jlm}$ and $d_{jlm}$ for $\mathfrak{su}(4)$. The structure constants for index combinations with $1 \leq j, l, m \leq 8$ in (57) and (59) for $\mathfrak{su}(4)$ are the same as $\mathfrak{su}(3)$ [32]. The additional values for $\mathfrak{su}(4)$ are given in (58) and (60).

| $C_{jlm} = \sqrt{2}$ | | $1/\sqrt{2}$ | $-1/\sqrt{2}$ | $\sqrt{6}/2$ |
|---|---|---|---|---|
| | 123 | 147 | 156 | 458 |
| | | 246 | 367 | 678 |
| $jlm$ | | 257 | | |
| | | 345 | | |

(57)

| $C_{jlm} = 1/\sqrt{2}$ | | $-1/\sqrt{2}$ | $1/\sqrt{6}$ | $-2/\sqrt{6}$ | $2/\sqrt{3}$ |
|---|---|---|---|---|---|
| | 1, 9, 12 | 1, 10, 11 | 8, 9, 10 | 8, 13, 14 | 9, 10, 15 |
| | 2, 9, 11 | 3, 11, 12 | 8, 11, 12 | | 11, 12, 15 |
| | 2, 10, 12 | 4, 10, 13 | | | 13, 14, 15 |
| | 3, 9, 10 | 6, 12, 13 | | | |
| $j, l, m$ | 4, 9, 14 | | | | |
| | 5, 9, 13 | | | | |
| | 5, 10, 14 | | | | |
| | 6, 11, 14 | | | | |
| | 7, 11, 13 | | | | |
| | 7, 12, 14 | | | | |

(58)

| $d_{jlm} = 2/\sqrt{6}$ | | $1/\sqrt{2}$ | $-1/\sqrt{2}$ | $-1/\sqrt{6}$ | $-2\sqrt{6}$ |
|---|---|---|---|---|---|
| | 118 | 146 | 247 | 448 | 888 |
| | 228 | 157 | 366 | 558 | |
| $jlm$ | 338 | 256 | 377 | 668 | |
| | | 344 | | 778 | |
| | | 355 | | | |

(59)

## ACKNOWLEDGMENT

This work was supported in part by the National Natural Science Foundation of China under Grant 61673264, Grant 61533012, Grant 61873162, and Grant 61973317, in part by the Australian Research Council Discovery Projects Funding Scheme under Project DP190101566, and in part by the Open Research Project of the State Key Laboratory of Industrial Control Technology, Zhejiang University, China, under Grant ICT2021B24.

## REFERENCES

[1] N. Gisin and R. Thew, "Quantum communication," *Nature Photon.*, vol. 1, no. 3, pp. 165–171, 2007, doi: 10.1038/nphoton.2007.22.

[2] M. A. Nielsen and I. L. Chuang, *Quantum Computation and Quantum Information*. Cambridge, U.K.: Cambridge Univ. Press, 2010.

[3] I. M. Georgescu, S. Ashhab, and F. Nori, "Quantum simulation," *Rev. Modern Phys.*, vol. 86, no. 1, pp. 153–185, 2014, doi: 10.1103/RevModPhys.86.153.

[4] N. Thomas Peter, B. J. Smith, A. Datta, L. Zhang, U. Dorner, and I. A. Walmsley, "Real-world quantum sensors: Evaluating resources for precision measurement," *Phys. Rev. Lett.*, vol. 107, no. 11, 2011, Art. no. 113603, doi: 10.1103/PhysRevLett.107.113603.

[5] C. Xiang, S. Ma, S. Kuang, and D. Dong. "Coherent $H^\infty$ control for linear quantum systems with uncertainties in the interaction Hamiltonian," *IEEE/CAA J. Autom. Sinica*, vol. 8, no. 2, pp. 432–440, Feb. 2021, doi: 10.1109/JAS.2020.1003429.

[6] L. Tan, D. Dong, D. Li, and S. Xue, "Quantum Hamiltonian identification with classical colored measurement noise," *IEEE Trans. Control Syst. Technol.*, vol. 29, no. 3, pp. 1356–1363, May 2021, doi: 10.1109/TCST.2020.2991611.

[7] D. Burgarth and K. Yuasa, "Quantum system identification," *Phys. Rev. Lett.*, vol. 108, no. 8, 2012, Art. no. 080502, doi: 10.1103/PhysRevLett.108.080502.

[8] C. Di Franco, M. Paternostro, and M. S. Kim, "Hamiltonian tomography in an access-limited setting without state initialization," *Phys. Rev. Lett.*, vol. 102, 2009, Art. no. 187203, doi: 10.1103/PhysRevLett.102.187203.

[9] J. Zhang and M. Sarovar, "Quantum Hamiltonian identification from measurement time traces," *Phys. Rev. Lett.*, vol. 113, no. 8, 2014, Art. no. 080401, doi: 10.1103/PhysRevLett.113.080401.

[10] A. Sone and P. Cappellaro, "Hamiltonian identifiability assisted by a single-probe measurement," *Phys. Rev. A*, vol. 95, no. 2, 2017, Art. no. 022335, doi: 0.1103/PhysRevA.95.022335.

[11] Y. Wang, D. Dong, A. Sone, I. R. Petersen, H. Yonezawa, and P. Cappellaro, "Quantum Hamiltonian identifiability via a similarity transformation approach and beyond," *IEEE Trans. Autom. Control*, vol. 65, no. 11, pp. 4632–4647, Nov. 2020, doi: 0.1109/TAC.2020.2973582.

[12] Y. Wang, D. Dong, B. Qi, J. Zhang, I. R. Petersen, and H. Yonezawa, "A quantum Hamiltonian identification algorithm: Computational complexity and error analysis," *IEEE Trans. Autom. Control*, vol. 63, no. 5, pp. 1388–1403, May 2018, doi: 10.1109/TAC.2017.2747507.

[13] I. De Vega and D. Alonso, "Dynamics of non-Markovian open quantum systems," *Rev. Modern Phys.*, vol. 89, no. 1, 2017, Art. no. 015001, doi: 10.1103/RevModPhys.89.15001.

[14] K.-D. Wu *et al.*, "Detecting non-Markovianity via quantified coherence: Theory and experiments," *npj Quantum Inf.*, vol. 6, no. 1, 2020, Art. no. 55, doi: 10.1038/s41534-020-0283-3.

[15] D. Burgarth and K. Yuasa, "Identifiability of open quantum systems," *Phys. Rev. A*, vol. 89, no. 3, 2014, Art. no. 030302, doi: 10.1103/PhysRevA.89.030302.

[16] H. Mabuchi, "Dynamical identification of open quantum systems," *Quantum Semiclassical Optics*: *J. Eur. Opt. Soc. B*, vol. 8, no. 6, 1996, Art. no. 1103, doi: 10.1088/1355-5111/8/6/002.

[17] J. Zhang and M. Sarovar, "Identification of open quantum systems from observable time traces," *Phys. Rev. A*, vol. 91, no. 5, 2015, Art. no. 052121, doi: 10.1103/PhysRevA.91.052121.

[18] Y. Kato and N. Yamamoto, "Structure identification and state initialization of spin networks with limited access," *New J. Phys.*, vol. 16, no. 2, 2014, Art. no. 023024, doi: 10.1088/1367-2630/16/2/023024.

[19] U. Weiss, *Quantum Dissipative Systems*, vol. 13. Singapore: World Scientific, 2012.

[20] R. Wu *et al.*, "Spectral analysis and identification of noises in quantum systems," *Phys. Rev. A*, vol. 87, no. 2, 2013, Art. no. 022324, doi: 10.1103/PhysRevA.87.022324.

[21] S. Xue, J. Zhang, and I. R. Petersen, "Identification of non-Markovian environments for spin chains," *IEEE Trans. Control Syst. Technol.*, vol. 27, no. 6, pp. 2574–2580, Nov. 2019, doi: 10.1109/TCST.2018.2879042.

[22] S. Krastanov, K. Head-Marsden, S. Zhou, S. T. Flammia, L. Jiang, and P. Narang, "Unboxing quantum black box models: Learning non-Markovian dynamics," 2020, *arXiv:2009.03902*.

[23] S. Krastanov, S. Zhou, S. T. Flammia, and L. Jiang, "Stochastic estimation of dynamical variables," *Quantum Sci. Technol.*, vol. 4, no. 3, 2019, Art. no. 035003, doi: 10.1088/2058-9565/ab18d5.

[24] M. Mohseni and D. A. Lidar, "Direct characterization of quantum dynamics," *Phys. Rev. Lett.*, vol. 97, 2006, Art. no. 170501, doi: 10.1103/PhysRevLett.97.170501.

[25] S. Bose, "Quantum communication through spin chain dynamics: An introductory overview," *Contemporary Phys.*, vol. 48, no. 1, pp. 13–30, 2007, doi: 10.1080/00107510701342313.

[26] H. P. Breuer, E. M. Laine, J. Piilo, and B. Vacchini, "Colloquium: Non-Markovian dynamics in open quantum systems," *Rev. Modern Phys.*, vol. 88, 2016, Art. no. 021002, doi: 10.1103/RevModPhys.88.021002.

[27] F. Shibata, Y. Takahashi, and N. Hashitsume, "A generalized stochastic Liouville equation. non-Markovian versus memoryless master equations," *J. Statist. Phys.*, vol. 17, no. 4, pp. 171–187, 1977, doi: 10.1007/BF01040100.

[28] S. Chaturvedi and F. Shibata, "Time-convolutionless projection operator formalism for elimination of fast variables. Applications to Brownian motion," *Ztschrift Für Phys. B Condens. Matter*, vol. 35, no. 3, pp. 297–308, 1979, doi: 10.1007/BF01319852.

[29] M. J. W. Hall, J. D. Cresser, L. Li, and E. Andersson, "Canonical form of master equations and characterization of non-Markovianity," *Phys. Rev. A*, vol. 89, 2014, Art. no. 042120, doi: 10.1103/PhysRevA.89.042120.

[30] E.-M. Laine, J. Piilo, and H.-P. Breuer, "Measure for the non-Markovianity of quantum processes," *Phys. Rev. A*, vol. 81, Jun. 2010, Art. no. 062115, doi: 10.1103/PhysRevA.81.062115.

[31] K. Lendi, "Evolution matrix in a coherence vector formulation for quantum Markovian master equations of $N$-level systems," *J. Phys. A: Math. Gen.*, vol. 20, no. 1, pp. 15–23, 1987, doi: 10.1088/0305-4470/20/1/011.

[32] R. Alicki and K. Lendi, *Quantum Dynamical Semigroups and Applications*, vol. 717. New York, NY, USA: Springer, 2007.

[33] S. Sastry, *Nonlinear Systems: Analysis, Stability, and Control*, vol. 10. New York, NY, USA: Springer, 1999.

[34] Q. Yu, Y. Wang, D. Dong, and I. R. Petersen, "On the capability of a class of quantum sensors," *Automatica*, vol. 129, 2021, Art. no. 109612, doi: 10.1016/j.automatica.2021.109612.

[35] J. H. Cole, S. G. Schirmer, A. D. Greentree, C. J. Wellard, D. K. Oi, and L. C. Hollenberg, "Identifying an experimental two-state Hamiltonian to arbitrary accuracy," *Phys. Rev. A*, vol. 71, no. 6, 2005, Art. no. 062312, doi: 10.1103/PhysRevA.71.062312.

[36] F. Niu, Z. O'Neill, and C. O'Neill, "Data-driven based estimation of HVAC energy consumption using an improved Fourier series decomposition in buildings," *Building Simul.*, vol. 11, no. 4, pp. 633–645, 2018, doi: 10.1007/s12273-018-0431-2.

[37] S. Chen, Z. Peng, Y. Yang, X. Dong, and W. Zhang, "Intrinsic chirp component decomposition by using Fourier series representation," *Signal Process.*, vol. 137, pp. 319–327, 2017, doi: 10.1016/j.sigpro.2017.01.027.

[38] A. R. Conn and Y. Li, "A structure-exploiting algorithm for nonlinear minimax problems," *SIAM J. Optim.*, vol. 2, no. 2, pp. 242–263, 1992, doi: 10.1137/0802013.

[39] S. Boyd and L. Vandenberghe, *Convex Optimization*. Cambridge, U.K.: Cambridge Univ. Press, 2004.

[40] I. Najfeld and T. F. Havel, "Derivatives of the matrix exponential and their computation," *Adv. Appl. Math.*, vol. 16, no. 3, pp. 321–375, 1995, doi: 10.1006/aama.1995.1017.

[41] G. Strang, "Karmarkar's algorithm and its place in applied mathematics," *Math. Intelligencer*, vol. 9, no. 2, pp. 4–10, 1987, doi: 10.1007/BF03025891.

[42] P. M. Vaidya, "An algorithm for linear programming which requires $O(((m+n)n^2+(m+n)^{1.5}n)l)$ arithmetic operations," *Math. Program.*, vol. 47, nos. 1–3, pp. 175–201, 1990, doi: 10.1007/BF01580859.

[43] P. M. Vaidya, "Speeding-up linear programming using fast matrix multiplication," in *Proc. 30th Annu. Symp. Found. Comput. Sci.*, 1989, pp. 332–337, doi: 10.1109/SFCS.1989.63499.

[44] Y. T. Lee and A. Sidford, "Efficient inverse maintenance and faster algorithms for linear programming," in *Proc. IEEE 56th Annu. Symp. Found. Comput. Sci.*, 2015, pp. 230–249, doi: 10.1109/FOCS.2015.23.

[45] M. B. Cohen, Y. T. Lee, and Z. Song, "Solving linear programs in the current matrix multiplication time," in *Proc. 51st Annu. ACM SIGACT Symp. Theory Comput.*, 2019, pp. 938–942, doi: 10.1145/3313276.3316303.

[46] H. P. Breuer and F. Petruccione, *The Theory of Open Quantum Systems*. London, U.K.: Oxford Univ. Press, 2002.

[47] M. D. Choi, "Completely positive linear maps on complex matrices," *Linear Algebra Appl.*, vol. 10, no. 3, pp. 285–290, 1975, doi: 10.1016/0024-3795(75)90075-0.

[48] S. Xue, L. Tan, M. Jiang, and D. Li, "A least squares identifier for a quantum non-Markovian environment model," *Quantum Inf. Process.*, vol. 18, no. 10, 2019, Art. no. 310, doi: 10.1007/s11128-019-2425-0.

**Shuixin Xiao** received the B.Eng. degree in automatic control from the Automation School, Huazhong University of Science and Technology, Wuhan, China, in 2018. He is currently working toward the Ph.D. degree in a joint Ph.D. program with Shanghai Jiao Tong University, Shanghai, China, and the University of New South Wales, Canberra, ACT, Australia.

His current research interests include quantum system identification, quantum computing, and quantum information processing.

**Shibei Xue** (Senior Member, IEEE) received the Ph.D. degree in control science and engineering from Tsinghua University, Beijing, China, in 2013.

He is currently an Associate Professor with the Department of Automation, Shanghai Jiao Tong University, Shanghai, China. From 2014 to 2016, he was a Postdoctoral Researcher with the University of New South Wales, Canberra, ACT, Australia, and then, he worked as a Postdoctoral Researcher with the Department of Physics, National Cheng Kung University, Tainan City, Taiwan. In July 2017, he joined Shanghai Jiao Tong University. His research interests include quantum control, optimization, and intelligent control of complex systems.

Dr. Xue was selected in Shanghai Pujiang Program funded by the Shanghai Science and Technology Committee in 2018. He is the Secretary-General of Quantum Control Theory and Technology Group in the Technical Committee on Control Theory of the Chinese Association of Automation.

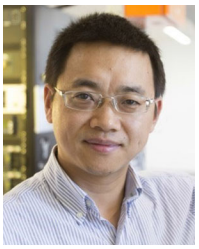

**Daoyi Dong** (Senior Member, IEEE) received the B.E. degree in automatic control and the Ph.D. degree in engineering from the University of Science and Technology of China, Hefei, China, in 2001 and 2006, respectively.

He is a currently the Scientia Associate Professor with the University of New South Wales, Canberra, ACT, Australia. He was with the Institute of Systems Science, Chinese Academy of Sciences, Guangzhou, China, and with the Institute of Cyber-Systems and Control, Zhejiang University, Hangzhou, China. He had visiting positions with Princeton University, Princeton, NJ, USA, RIKEN, Wako-Shi, Japan, University of Duisburg-Essen, Duisburg, Germany, and The University of Hong Kong, Hong Kong. His research interests include quantum control and machine learning.

Dr. Dong received an ACA Temasek Young Educator Award by The Asian Control Association. He is a recipient of an International Collaboration Award, a Humboldt Research Fellowship from the Alexander von Humboldt Foundation of Germany, and an Australian Postdoctoral Fellowship from the Australian Research Council. He serves as an Associate Editor for IEEE TRANSACTIONS ON NEURAL NETWORKS AND LEARNING SYSTEMS and a Member-at-Large on the Board of Governors of the IEEE Systems, Man, and Cybernetics Society. He was the General Chair of the 1st Quantum Science, Engineering and Technology Conference.

**Jun Zhang** (Senior Member, IEEE) received the B.S. degree in automatic control from Shanghai Jiao Tong University, Shanghai, China, in 1993, and the M.S. and Ph.D. degrees in electrical engineering from the University of California at Berkeley, Berkeley, CA, USA, in 1999 and 2003, respectively.

He was a Research Specialist with the Department of Berkeley Chemistry and also a Staff Engineer at several high tech firms in the Silicon Valley. He is currently a Professor with the UMich–SJTU Joint Institute, Shanghai Jiao Tong University. His current research interests include quantum control, process, and motion control.